Sensor signal processing

Radar Target Classification Based on High Resolution Range Profile Segmentation and Ensemble Classification

Jia Liu[1] and Qunyu Xu[2]

[1]Research Institute for Frontier Science, Beihang University, Beijing 100191, China
[2]Research Institute of Civil Aviation Law, Regulation and Standardization, China Academy of Civil Aviation Science and Technology, Beijing 100028, China

Manuscript received February 22, 2021; accepted March 5, 2021. Date of publication March 17, 2021; date of current version April 12, 2021.

Abstract—Radar target range profile possesses advantages in many target recognition problems. Feature extraction techniques could optimize target recognition performance, but conventional methods neglect specific characters of electromagnetic scattering mechanisms in range profiles. This letter introduces a range profile segmentation algorithm, which decomposes target range profile into segments corresponding to particular electromagnetic scattering mechanisms. Segment type identification and weighing algorithms are also developed for ensemble classification strategy. Results indicate that the proposed method could achieve comparable classification accuracy as advanced neural networks but requires far fewer computational resources to guarantee its application flexibility.

Index Terms—Sensor signal processing, feature extraction, radar target recognition, range profile, wavelet decomposition.

I. INTRODUCTION

The high resolution range profile (HRRP) is an effective radar target signature in various noncooperative radar automatic target recognition (RATR) problems. Many works in this area have been trying to enhance target classification accuracy and performance [1], [2]. Classification methods using HRRP evolve from early template matching to machine learning techniques like convolutional neural networks (CNNs) [3]. Besides classification methods, other factors have dominant impact on classification performance, such as range profile quality and feature extractions. In many application scenarios, the direct application of range profile characters provides unexpected classification performance. Therefore, effective HRRP feature extraction is a major research topic in HRRP-RATR problems.

Projecting original range profile signatures into another space are commonly adopted in this area. Existing works well handle various target range profiles in the feature space [4], [5] to accommodate practical application requirements. However, these works usually consider range profiles in a general manner as in generalized classification problems. Unique physical essences of range profiles are not well explored and utilized. As a radial dimensional electromagnetic scattering descriptor, the scattering intensity within a specific range bin and its relative position contains distinguishable target characters, which are not comprehensively considered in existing feature extraction techniques. The specific intensity distribution pattern usually has close relevance with electromagnetic scattering mechanism [6]. Existing methods manipulate range profiles as integrated feature vectors, and different electromagnetic scattering mechanisms are evaluated in an unbiased approach, which is against physical essence of electromagnetic scatterings for target recognition. Dominant scattering mechanisms are not sufficiently utilized while the minor scattering mechanism over contributes to classification. If electromagnetic scattering mechanisms could be recognized in range profiles and manipulated properly, better classification accuracy could be expected. Moreover, the increasing radar range resolution provides higher dimensional range profile feature vectors with larger computational burden. Dimension reduction techniques reduce information redundancy but also result in inevitable information loss. An effective dimension reduction technique for range profile feature vectors is promising to further optimize classification performance.

This letter introduces a novel range profile segmentation method and an ensemble classification strategy. Range profile segments have close relevance with electromagnetic scattering mechanisms and a specific weighing algorithm reasonably quantifies their contributions in ensemble classification. Fuzzy-support vector machine (SVM) is adopted as the classifier and provides probabilistic class membership for cooperation with weighing factors. Results of aircraft classification verify the proposed method's accuracy and expected efficiency optimization to consolidate its application significance.

II. HRRP SEGMENTATION AND WEIGHING

A. Electromagnetic Scattering Mechanism Discussion

A target range profile is interpreted as a series of range bins with scattering intensity information. All scatterers' contributions within each range bin are coherently integrated into a scattering intensity value. Electromagnetic scattering mechanisms are reflected from a scattering intensity value as well as variation patterns from neighboring bins. For bins with high intensity and smooth variation characters, a corresponding electromagnetic scattering mechanism is usually the specular reflection from large flat planes, corner structures, or inlets. Bins with medium scattering intensity and prominent oscillations usually indicate composition scattering from multiple objects with comparable size of radar wavelength with resonance scattering effects. Range bins with minor scattering intensities and smooth variation patterns indicate no dominant scatterers, and corresponding mechanism is usually weak electromagnetic scattering effects like diffraction or travelling waves. Based on scattering mechanism analysis, combined with attitude and range bin information, target size and geometry characters might be deduced. Among scattering mechanisms, specular reflections are

Corresponding author: Jia Liu (e-mail: bobmp5@163.com).
Associate Editor: F. Costa.
Digital Object Identifier 10.1109/LSENS.2021.3066596

dominant in classification and contain most distinguishable features. In contrast, minor and smooth scattering intensity patterns in range profiles contain limited distinguishable features. These features' contributions should be respectively considered in classification instead of being integrated into an unbiased feature space. As electromagnetic scattering mechanisms are usually reflected within a partially consecutive segment, it is reasonable to divide range profiles into segments for electromagnetic scattering mechanism interpretation.

B. Range Profile Segmentation Procedure

A range profile segment database with manually labeled electromagnetic scattering mechanisms is constructed for automatic identification of electromagnetic scattering mechanism types. Statistical analyses assisted by visual evaluations are applied in the database, and an HRRP segmentation algorithm using wavelet decomposition and statistical similarity description is proposed.

The physical essence of electromagnetic scattering mechanisms is described in specific multiscale distribution characters. Wavelet methods [7] are good at providing multiresolution data analysis in spatial-temporal domain, which makes the wavelet decomposition method widely used in many signal segmentation methods. For a range profile, scattering intensities are represented by a vector $\boldsymbol{h} = [h_1, h_2, \ldots, h_L]$, in which L denotes the number of effective range bins. In the segmentation procedure, $\boldsymbol{h}$ is equally divided into K segments denoted as $\boldsymbol{h}_k$. These segments are merged based on mutual similarities. A segment $\boldsymbol{h}_k$ is decomposed by wavelet transformation

$$\boldsymbol{h}_k = \sum_{j=1}^{M} e_{j,k}\boldsymbol{\Phi}_{j,k} + \sum_{i=1}^{N} d_{i,k}\boldsymbol{\Psi}_{i,k}. \tag{1}$$

The term $\boldsymbol{E}_k = \sum_{j=1}^{M} e_{j,k}\boldsymbol{\Phi}_{j,k}$ represents the global field of $\boldsymbol{h}_k$ as envelop patterns. The vector $\boldsymbol{\Phi}_{j,k}$ is the scaled element of wavelet family. The second term $\boldsymbol{D}_k = \sum_{i=1}^{N} d_{i,k}\boldsymbol{\Psi}_{i,k}$ denotes the local field of $\boldsymbol{h}_k$ as oscillation patterns. The vector $\boldsymbol{\Psi}_{i,k}$ is the translate element of wavelet family. M and N denote wavelet decomposition level in scaled and translate dimensions. Segment differences are evaluated by considering both global and local fields. The global field evaluation is in Hilbert space

$$\overline{\boldsymbol{S}}_{j,k} = \sqrt{\left(\boldsymbol{E}_{j,k}\right)^2 + \left(\hat{\boldsymbol{E}}_{j,k}\right)^2}. \tag{2}$$

$\hat{\boldsymbol{E}}_{j,k}$ indicates the Hilbert transform. The global field difference is

$$S^d\left(\boldsymbol{h}_k, \boldsymbol{h}_{k+1}\right) = \frac{K}{L\cdot(M-1)} \sum_{j=1}^{M-1} \left\| \overline{\boldsymbol{S}}_{j,k} - \overline{\boldsymbol{S}}_{j,k+1} \right\|_1 \tag{3}$$

in which $\| \bullet \|_1$ indicates the L − 1 norm of a vector. The KL divergence is taken in local field evaluation to describe the statistical difference of high frequency components. The original definition of KL divergence is

$$KL(\boldsymbol{P}, \boldsymbol{Q}) = \sum_{r} p(r) \log\left(p(r)\big/(p(r)/2 + q(r)/2)\right). \tag{4}$$

Symbols $p(r)$ and $q(r)$ indicate probability density function of $\boldsymbol{P}$ and $\boldsymbol{Q}$. The local field difference is the averaged KL divergence

$$KL^{\text{avg}}(\boldsymbol{h}_k, \boldsymbol{h}_{k+1}) = KL(\boldsymbol{D}_k, \boldsymbol{D}_{k+1})\big/(N-1). \tag{5}$$

Normalized weighing factor is used in overall evaluation

$$T\left(\boldsymbol{h}_k, \boldsymbol{h}_{k+1}\right) = w_e \cdot S^{*d}\left(\boldsymbol{h}_k, \boldsymbol{h}_{k+1}\right) + w_{KL} \cdot KL^{*\text{avg}}\left(\boldsymbol{h}_k, \boldsymbol{h}_{k+1}\right). \tag{6}$$

Values of weighing parameters w_e and w_h are dependent on range profile characters; the symbol $*$ indicates normalized descriptors. The segmentation procedure starts from $\boldsymbol{h}_1$ as an initial segment, and the segment merging is applied consecutively. Whether segment $\boldsymbol{h}_k$ should be merged with its previous segments $\boldsymbol{J}_l$ depends on their overall difference by following criterion:

$$\begin{cases} \boldsymbol{J}_l = \{\boldsymbol{J}_l, \boldsymbol{h}_k\} & T\left(\boldsymbol{J}_l, \boldsymbol{h}_k\right) < \sigma \\ \boldsymbol{J}_{l+1} = \boldsymbol{h}_k & T\left(\boldsymbol{J}_l, \boldsymbol{h}_k\right) > \sigma \end{cases}. \tag{7}$$

The parameter σ is the threshold whose value has close relevance with radar bandwidth. In this article, σ ranges from 0.2 to 0.8.

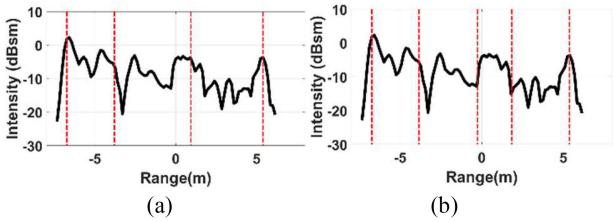

Fig. 1. HRRP segmentation illustration for aircraft range profile. (a) Three segments. (b) Four segments.

C. Range Profile Segment Type Identification

Automatic range profile segment type identification is conducted by defining a series of segment descriptors including mean of data m, total number of max point $N_{\max}$, and maximum point series $\boldsymbol{P}_{\max}$. $R(\boldsymbol{h})$ indicates the range of scattering intensity. The peak segment type corresponds to dominant scattering mechanism and is identified from

$$\begin{cases} P_{\text{peak}} \subseteq \boldsymbol{P}_{\max} \\ P_{\text{peak}} - \boldsymbol{P}_{\max}(k+1) > \delta_{\text{peak}} \times R\left(\boldsymbol{h}\right) \\ P_{\text{peak}} - \boldsymbol{P}_{\max}(k-1) > \delta_{\text{peak}} \times R\left(\boldsymbol{h}\right) \end{cases} \tag{8}$$

where P_{peak} denotes a peak point value. The parameter δ_{peak} is defined as 0.2. The oscillation segment type corresponds to the resonance scattering mechanism with prominent peak and trough points in an oscillation pattern. The mean value of oscillation segment is close to its median value with large standard deviation

$$\begin{cases} |m-u| < \delta_{\text{mean}} \times R\left(\mathbf{h}\right) \\ \chi_{\text{osc}} \geq \delta_{\text{std}} \times R\left(\mathbf{h}\right) \end{cases} \tag{9}$$

in which δ_{mean} is 0.2, indicating the mean value deviation from median value u should be within 20%. χ_{osc} indicates the oscillation range. The standard deviation parameter δ_{std} is 0.5, indicating that the intensity oscillation should be larger than 50% of the intensity range. Segments excluding peak and oscillation ones are categorized as usual segment type. These segments do not contain dominant scattering points with smooth variation patterns corresponding to minor electromagnetic scatterings. Fig. 1 presents an aircraft range profile segmentation example into three and four segments. Dominant peak segments are extracted from first a few range bins corresponding to inlet structure. The oscillation segment is extracted in both cases with slight boundary difference. The difference between three and four segments is mainly reflected on usual segments.

III. ENSEMBLE CLASSIFICATION STRATEGY

A. Ensemble Classification Strategy

Several lower dimensional training databases and sub classifiers are constructed according to training range profile segment types for ensemble classification strategy. In classification, an unknown

target range profile is segmented and distributed in respective sub classifiers. The target classification result is based on the voting of weighed class membership from all sub classifiers. In this letter, the fuzzy-SVM learning machine [8] is adopted to provide a quantitative class membership evaluation for all candidate classes.

B. Weighing Factor Definition

A novel weighing factor definition is proposed to quantitatively accommodate different segment type contribution in classification. For peak segments, the weighing factor is defined as

$$w_p = \sum_{i=1}^{N_P} \frac{\left|\boldsymbol{E}_p(i)\right|}{\boldsymbol{R}(i)} \tag{10}$$

in which $\boldsymbol{E}_p(i) = 10^{\boldsymbol{J}_p(i)/10}$, $\boldsymbol{J}_p(i)$ is the amplitude of peak point i in the segment, $\boldsymbol{R}(i)$ is the width of the peak point i using 3 dB criterion, and N_p denotes the total number of peak points. For oscillation segments, weighing factor should be able to reflect intensity fluctuation characters, which is dependent on mean energy and frequency spectra

$$w_o = \sum_{i=1}^{N_o} \frac{1}{\boldsymbol{R}_o(i)} \left(\boldsymbol{E}_o(i) + \boldsymbol{Y}_o(i)\right) \tag{11}$$

in which $\boldsymbol{Y}_o(i) = \|FFT(\boldsymbol{J}_o)\|$. $\boldsymbol{E}_o(i)$ and $\boldsymbol{R}_o(i)$ take the similar definition as in (10). Usual segments do not exhibit prominent characters in amplitudes and oscillations, and their weighing factor is defined as

$$w_u = \sum_{i=1}^{N_u} \frac{1}{2\boldsymbol{R}_u(i)} \left(\boldsymbol{E}_u(i) + \boldsymbol{Y}_u(i)\right). \tag{12}$$

Parameter definitions in (12) are similar to other two segment types. Weighing factor definitions for three segment types are based on the same principle, which is the ratio between electromagnetic scattering energy and its width. Segments with larger scattering energy and clustering character is assigned with larger weigh factors to consolidate their significance in classification, which is consistent with the physical essence in target classification.

C. Target Class Determination

For an unknown range profile $\boldsymbol{h}$ decomposed into Q segments $\boldsymbol{h}_i (i = 12,..Q)$, each fuzzy-SVM classifier in the ensemble classification system provides a class membership description

$$\boldsymbol{P}(\boldsymbol{h}) = \{\boldsymbol{p}(h_i) \,|i = 1, 2, \ldots, Q\}. \tag{13}$$

The vector $\boldsymbol{p}(\boldsymbol{h}_i) = [p^1(\boldsymbol{h}_i), p^2(\boldsymbol{h}_i), \ldots, p^C(\boldsymbol{h}_i)]$ contains class membership degree of C classes, and $p^j(\boldsymbol{h}_i)$ is the membership degree of class j for segment $\boldsymbol{h}_i$. Membership degree is defined between 0 and 1 with larger value indicate higher probability of belonging to a class. The weighed class membership degree is

$$\boldsymbol{P}^w(\boldsymbol{h}) = \{w_i \cdot \boldsymbol{p}(h_i) \,|i = 1, 2, \ldots, Q\}. \tag{14}$$

Weighing factors defined in (10)–(12) are normalized in (14). The summation of weighed class membership degree for class j is

$$X^j(\boldsymbol{h}) = \sum_{i=1}^{Q} w_i \cdot \boldsymbol{p}(\boldsymbol{h}_i). \tag{15}$$

The class with maximum $X^j(\boldsymbol{h})$ value is the final class decision

$$c(\boldsymbol{h}) = \arg\max_j \left\{X^j(\boldsymbol{h})\right\}. \tag{16}$$

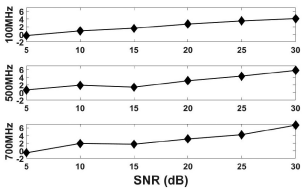

Fig. 2. Classification accuracy differences pattern with SNR.

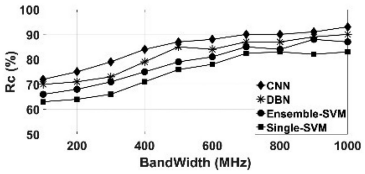

Fig. 3. Accuracy comparison of classification methods.

As peak segments contain more distinguishing characters for classification, class membership degree from corresponding classifiers possess higher accuracy. The larger weighing factor from (10) further emphasizes its contribution. In contrast, there exists higher uncertainties in class membership degree for usual segments due to limited distinctive classification features. The smaller weighing factor refrains this uncertainty in classification. Therefore, the overall class decision theoretically possesses better accuracy.

IV. RESULTS AND DISCUSSION

Four aircraft models are employed to verify the proposed method. Geometry details of aircraft targets are described in [9]. Range profiles are generated from simulation platforms based on the graphical electromagnetic computing method [9]. The computer is configured with Intel Core i5-3470 CPU and 8 GB random access memory (RAM). The fuzzy-SVM classifier comes from the LIBrary of SVM (LIBSVM) [11] toolbox. Attitude angles are randomly sampled in azimuth and elevation planes within $[-10^o, 10^o]$ and $[-5^o, 5^o]$ to build training and testing databases, which contain 5147 and 842 samples, respectively, with repetition rate of 1.67%. The central frequency of the radar is 9.85 GHz with bandwidth ranging from 100 MHz to 1 GHz. The radar takes vertical transmitting and reception polarization. Environmental noises are considered in signals with signal-to-noise ratio (SNR) ranging from 5 to 20 dB.

A. Classification Accuracy

The rate of correct classification R_c is employed as an accuracy descriptor. Fig. 2 presents R_c differences over SNR ranging from 5 to 30 dB in three bandwidths. Positive value indicates better accuracy of the ensemble classification method compared with a single fuzzy-SVM classifier. R_c difference is not prominent in the low SNR regime. The slight accuracy improvement is contributed by smaller weighing factor in usual segments. The accuracy advantage gets prominent with increasing SNR as dominant scattering mechanisms are emphasized while noise interference is refrained. Results are compared with CNNs and deep belief networks methods with details depicted in [3] and [10]. R_c distributions are presented in Fig. 3 with SNR of 20 dB. The confusion matrix in Table 1 illustrates detailed classification accuracy between ensemble classification and CNN in 300 and 800 MHz bandwidths. The CNN possesses supreme classification capability for its better robustness in translation and rotation invariance. The ensemble

Table 1. Confusion Matrix Comparison Between CNN and Ensemble Classification Methods (Ensemble Classification/CNN).

	300MHz				800MHz			
	A	B	C	D	A	B	C	D
A	68/76	19/12	10/8	3/4	79/88	12/7	6/4	3/1
B	21/14	70/77	5/6	4/3	11/6	82/88	5/2	2/4
C	9/7	14/9	71/80	6/4	6/4	5/3	86/91	3/2
D	5/4	8/6	12/7	75/83	3/3	5/2	3/2	89/93

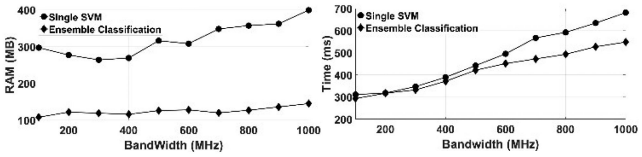

(a) (b)

Fig. 4. Efficiency evaluation of the proposed method. (a) RAM. (b) Time.

classification method has comparable accuracy but requires much lower computational costs and possess better flexibility on sampling database.

B. Classification Efficiency

Efficiency performance is evaluated from averaged RAM consumption in training and average time consumption in classification. The RAM consumption includes feature vector storage and classification hyperplane construction. As neural network methods require much more resources, the efficiency evaluation is compared between fuzzy-SVM classifiers, as in Fig. 4(a). Time consumption in Fig. 4(b) indicates the averaged classification time for one unknown range profile. There reflects the nonlinear RAM consumption with feature dimension in SVM. This character results in lower RAM consumption for ensemble classification under the same feature dimension, which is more prominent in higher bandwidths. More classification time is required with higher dimensional features caused by increasing radar bandwidth for both methods, as illustrated in Fig. 4(b). For ensemble classification, an extra segmentation procedure is applied on each test range profile, and several classification operations are performed. Due to the nonlinear time consumption in classification, multiple classification operations neutralize reduced dimension of classifiers, leading to similar time consumption in lower bandwidths. However, the classification time benefit gets prominent in higher bandwidths due to increased range profile complexity. In ensemble classification, fuzzy-SVM classifiers possess most computational resources. The general computational complexity for SVM is $O(N^3)$. Therefore, the overall computational complexity is mainly dependent on the dominant segment dimension.

C. Existing Problems

The current method is limited to small attitude sampling scope. Broad target attitude would lead to inconsistent segment type and dimensions, which brings extra complexities in classification system construction. Therefore, the current method is not applicable to more generalized RATR problems but confined to particular target classification scenario with small attitude variation scopes. More flexible segmentation and classification strategy under larger attitude sampling scopes would be the future work to extend its generality.

V. CONCLUSION

Feature extraction techniques are increasingly important in HRRP-RATR problems. Existing techniques consider range profiles as generalized feature vectors, and electromagnetic scattering mechanism exploration is usually neglected. This letter introduces a novel HRRP segmentation as well as a segment type identification method to extract characters of target electromagnetic scattering mechanisms. Specific weighing factor evaluation and ensemble classification strategy are also developed. The proposed method could emphasize contributions from dominant electromagnetic scatterings while refraining from unimportant contributions. Classification results indicate the proposed method has comparable classification accuracy as advanced neural networks with much less resource consumption to guarantee efficiency and flexibility in practical application scenarios.

REFERENCES

[1] O. Karabayir, U. Saynak, M. Z. Kartal, A. F. Coskun, and B. Bati, "Synthetic range profile-based training library construction for ship target recognition purposes of scanning radar systems," *IEEE Trans. Aerosp. Electron. Syst.*, vol. 56, no. 4, pp. 3231–3245, Aug. 2020.

[2] J. Liu, N. Fang, Y. J. Xie, and B. F. Wang, "Radar target classification using support vector machine and subspace methods," *IET Radar Sonar Navigation*, vol. 9, no. 6, pp. 632–640, 2015.

[3] Y. Wen, L. Shi, X. Yu, Y. Huang, and X. Ding, "HRRP target recognition with deep transfer learning," *IEEE Access*, vol. 8, pp. 57859–57867, Mar. 2020.

[4] P. Guo, Z. Liu, and J. Wang, "HRRP multi-target recognition in a beam using prior-independent DBSCAN clustering algorithm," *IET Radar, Sonar Navigation*, vol. 13, no. 8, pp. 1366–1372, 2019.

[5] J. Wang, Z. Liu, L. Ran, and R. Xie, "Feature extraction method for DCP HRRP-based radar target recognition via m − χ decomposition and sparsity-preserving discriminant correlation analysis," *IEEE Sensors J.*, vol. 20, no. 8, pp. 4321–4332, Apr. 2020.

[6] H. Fan, Y. Peng, Z. Feng, X. Shan, and D. Lu, "Interpreting scattering mechanism of radar target by wavelet transform," in *Proc. Int. Radar Conf.*, 1995, pp. 416–418.

[7] M. Mesarcik, S. Lewis, A. Mishra, J. Pidanic, and K. Juryca, "Discrete wavelet design for target classification in pulse-doppler surveillance radar," in *Proc. 29th Int. Conf. Radioelektronika (RADIOELEKTRONIKA),* Apr. 2019, pp. 1–6.

[8] J. Liu, N. Fang, Y. J. Xie, and B. F. Wang, "Multi-scale feature-based fuzzy-support vector machine classification using radar range profiles," *IET Radar Sonar Navigation*, vol. 10, no. 2, pp. 370–378, 2016.

[9] J. Liu and B. F. Wang, "Dynamic aircraft identification using hrrp under attitude perturbation interference," *J. Electromagn Waves Appl.,* vol. 33, no. 7, pp. 929–945, 2019.

[10] G. E. Hinton and R. R. Salakhutdinov, "Reducing the dimensionality of data with neural networks," *Science*, vol. 313, no. 5786, pp. 504–507, 2006.

[11] C. C. Chang and C. J. Lin, "LIBSVM: A library for support vector machines," *ACM Trans. Intell. Syst. Technol.*, vol. 2, no. 3, 2011, Art. no. 27.